

# MEASUREMENT OF SMALL FLOW RATES THROUGH RADIAL CLEARANCES

**Darko KNEŽEVIĆ<sup>\*1</sup>, Saša LALOŠ<sup>1</sup>, Jovan ŠKUNDRIĆ<sup>1</sup>, Zdravko MILOVANOVIĆ<sup>1</sup>, Dejan BRANKOVIĆ<sup>1</sup>**

<sup>1</sup> Faculty of Mechanical Engineering, University of Banja Luka, Banja Luka, Bosnia and Herzegovina

<sup>\*</sup> Corresponding author; E-mail: darko.knezevic@mf.unibl.org

*In most hydraulic components, small orifices and clearances of various geometric shapes govern their operation and influence the components and the hydraulic system's efficiency and dynamic behavior. In applications requiring precise actuator positioning with small and rapid movements, mathematical modeling of fluid flow in control valves (such as servo valves and load-sensing regulators) becomes particularly important. A critical part of this modeling is accurately describing fluid flow through small orifices, especially radial clearances.*

*The most important physical properties of fluids that affect flow through small orifices are density and dynamic viscosity. This paper presents the theoretical basis for determining the change in density and dynamic viscosity of mineral hydraulic oils as a function of the thermodynamic state (pressure and temperature), then gives an analytical expression for determining the flow rate through so-called long radial clearances taking into account the thermodynamic state of the working fluid, and finally describes the installation for experimental measurement of flow rate through small orifices (in the specific case of radial clearances).*

**Key words:** Small flow rate, measurement, orifice, radial clearance

## 1. Introduction

Small orifices and clearances in hydraulic components serve multiple functions. Nozzles integrated within components enable control of operation – for example, in indirectly controlled pressure and flow valves. Internal clearances facilitate the relative motion of component elements, enabling the realization of specific functions. Moreover, these clearances ensure sealing between regions of different pressures and can serve as hydrostatic or hydrodynamic bearings, depending on the internal force distribution. As a result, the optimization of a hydraulic component is often centered on optimizing its internal clearances.

The flow rate through small orifices (nozzles) and clearances in hydraulic components is influenced by several factors:

- the geometry of the orifice (nozzle) or clearance,
- the operating temperature of the hydraulic system,
- the working pressure,
- the fluid's viscosity, which itself depends on temperature, pressure, and the type of hydraulic fluid used.

Previous research related to small clearances flow has primarily focused on modeling, numerical simulations, or experimental measurement of hydraulic components cumulative leakage.

Dziubak et al. [1] analyzed internal leakage through radial clearances in spool valves used in automatic transmissions. A leakage model was developed to describe the flow, taking into account the effects of wear on clearance size and the impact of increased operating temperature – i.e., reduced viscosity on leakage flow. However, the influence of clearance length and pressure on the magnitude of internal leakage was not addressed.

The authors of [2], [3] investigated the influence of internal leakage through clearances on the efficiency of internal curve hydraulic motors. Their study was based on CFD simulations and experimental methods for measuring cumulative internal leakage. The analysis examined the impact of rotational speed, temperature, inlet pressure, and viscosity, as well as the dimensions of individual clearances, on leakage behavior.

The study presented in [4] examined the effect of blade tip clearance in vane pumps on cavitation and two-phase flow phenomena. The research, conducted through numerical simulations, demonstrated that increasing the clearance reduces volumetric efficiency and amplifies pressure pulsations, particularly under two-phase (gas-liquid) flow conditions. These findings highlight that even minimal changes in radial clearances can drastically alter flow behavior in components operating at high rotational speeds.

Peng et al. [5] investigated the influence of end and radial clearances on the overall efficiency of a high-speed gear pump. The research, based on numerical simulations, analyzed the input shaft power and leakage flow across a range of clearance values. Optimal dimensions of axial and radial clearances were identified to maximize the pump's overall efficiency.

The influence of radial and axial clearance on the volumetric efficiency of a external gear pump was also examined in [6]. The study presents results obtained via CFD simulations, evaluating internal leakage as a function of clearance size and geometry under various operating parameters. The simulation results were compared with experimental measurements of volumetric efficiency, although no direct leakage measurements were conducted through the clearances.

Li and Wu [7] investigated the leakage mechanism through radial clearances between the piston and housing of hydraulic components operating under extreme deep-sea conditions. They developed a theoretical leakage model that accounts for elastic deformation of the clearance geometry due to high ambient and working pressures, pressure-induced viscosity increase, temperature effects, as well as eccentricity and tilt of the moving parts. Their results demonstrated that classical models can significantly overestimate leakage, by up to five times due to the neglect of these effects. Based on their analysis, a criterion for the minimum clearance size was proposed to strike a balance between sealing effectiveness and mobility of moving elements. However, no experimental validation of the model was performed.

The existing research highlights the crucial role of radial clearances in ensuring the proper functioning and reliability of hydraulic components, particularly in terms of leakage control, sealing, lubrication, and overall energy efficiency. Most studies emphasize idealized geometries and numerical analyses, while experimental investigations under realistic conditions, especially for very small flow rates and clearances, remain limited. Despite advances in modern simulation techniques, there is still a strong demand for accurate experimental data to validate theoretical models.

In the present study, the analysis focuses on small orifices in the form of radial clearances, which represent the most common orifice type in hydraulic control and regulation components. Experimental measurements of small flow rates through radial clearances were conducted under controlled laboratory conditions, with precise temperature and pressure regulation. A dedicated experimental setup designed for this purpose is also presented.

## 2. Mathematical Modeling of Hydraulic Fluid Physical Properties Depending on the Thermodynamic State

The physical properties of hydraulic fluids, particularly density and viscosity, play a crucial role in determining the efficiency and dynamic behavior of hydraulic components and systems. Density directly affects pressure drop and, consequently, energy losses. A higher-density fluid requires more power for circulation and exhibits a slower response in unsteady operating conditions. Moreover, higher density increases the risk of cavitation, erosion, and sudden pressure surges during flow variations. Dynamic viscosity also influences pressure drop, volumetric losses, and the formation of a lubricating film. A fluid with higher viscosity reduces leakage through clearances, improves sealing, and increases mechanical losses. In comparison, lower viscosity leads to a thinner lubricating layer and a greater risk of wear.

Since density and dynamic viscosity vary with the thermodynamic state (pressure and temperature), this relationship is essential for precisely characterizing hydraulic fluids in real operating environments.

### 2.1. Density of Hydraulic Fluids

Unlike the corresponding equation for gases, the thermal equation of state for liquids does not have a direct analytical derivation from fundamental physical laws:

$$d\rho = \left( \frac{\partial \rho}{\partial T} \right)_p dT + \left( \frac{\partial \rho}{\partial p} \right)_T dp \quad (1)$$

where:

$\rho$  – density [kg/m<sup>3</sup>];

$T$  – relative temperature [°C];

$p$  – absolute pressure [Pa].

From Eq. (1) two important coefficients can be defined:

$$\alpha_p = -\frac{1}{\rho} \left( \frac{\partial \rho}{\partial T} \right)_p \quad (2)$$

$$K_T = \rho \left( \frac{\partial p}{\partial \rho} \right)_T \quad (3)$$

In Eq. (2),  $\alpha_p$  [°C<sup>-1</sup>] represents the volume-temperature expansion coefficient, and in Eq. (3),  $K_T$  [Pa] represents the isothermal bulk modulus.

Fig. 1 presents experimental data illustrating the variation in density of mineral hydraulic oil HM 46 with pressure and temperature [8].

The density of mineral oil at a given temperature and atmospheric pressure can be estimated using the experimentally measured density at 15 °C ( $\rho_0$ ) and the volume-temperature expansion coefficient ( $\alpha_p$ ) at the same reference temperature. The relationship is given by the Eq. (4) [8]:

$$\rho = \rho_0 - \rho_0 \alpha_{p0} (T - 15) = \rho_0 [1 - 0.0007 (T - 15)] \quad (4)$$

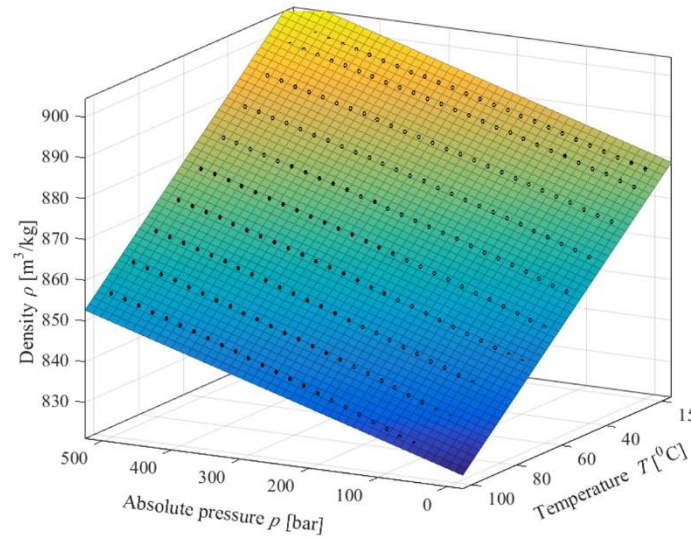


**Figure 1. Variation of density of mineral hydraulic oil HM 46 on the dependence of thermodynamics state**

## 2.2. Temperature Dependence of Viscosity

The viscosity of hydraulic and lubricating oils is highly sensitive to temperature. As the temperature increases, the viscosity decreases rapidly.

Several equations have been developed to describe the relationship between viscosity and temperature. These equations range from purely empirical formulations to those based on theoretical models. Tab. 1 presents the most commonly used equations in hydraulic fluid modeling [9].

**Table 1. Viscosity-temperature equations**

Name	Equation	Comments
Reynolds	$\mu_0 = be^{-aT_A}$	One of the earliest equations; accurate only over a narrow temperature range.
Slotte	$\mu_0 = \frac{a}{(b + T_A)^c}$	Reasonably accurate; suitable for numerical analysis.
Walther	$(\nu_0 + a) = bd^{\frac{1}{T_A^c}}$	Basis of the ASTM viscosity-temperature chart.
Vogel	$\mu_0 = ae^{\frac{b}{(T_A - c)}}$	High accuracy; widely used in engineering calculations.

where:

$a, b, c, d$  – are empirical constants specific to each model;

$\mu_0$  – dynamic viscosity at atmospheric pressure [Pa·s];

$\nu_0$  – kinematic viscosity at atmospheric pressure [m<sup>2</sup>/s];

$T_A$  – absolute temperature [K].

Among the listed models, the Vogel equation is considered the most accurate for practical engineering calculations. [9].

### 2.3. Pressure Dependence of Viscosity

The viscosity of hydraulic oils increases with pressure. This pressure-viscosity behavior is strongly influenced by the chemical composition of the fluid.

The most widely used model to describe this behavior is the Barus equation [10]:

$$\mu = \mu_0 e^{\alpha p} \quad (5)$$

where:

$\mu$  – dynamic viscosity at the pressure  $p$  [Pa·s];

$\alpha$  – pressure-viscosity coefficient, which depends on the thermodynamic state of the fluid [Pa<sup>-1</sup>].

### 2.4. Dynamic Viscosity as a Function of Temperature and Pressure for Mineral Hydraulic Oils

The Vogel equation is commonly used to describe the temperature dependence of dynamic viscosity at atmospheric pressure. It is expressed as:

$$\mu(T) = \mu_0 = a e^{\left[ \frac{b}{(T+273.15)-c} \right]} \quad (6)$$

To account for both temperature and pressure effects, the Vogel equation Eq. (6) can be substituted into the Barus equation Eq. (5), resulting in a combined model for dynamic viscosity under varying thermal and pressure conditions Eq (7):

$$\mu(p, T) = a e^{\left[ \frac{b}{(T+273.15)-c} \right]} e^{\left[ \frac{p}{a_1 + a_2 T + (b_1 + b_2 T) p} \right]} \quad (7)$$

This results in an equation with seven unknown parameters –  $a, b, c, a_1, a_2, b_1$  and  $b_2$  – all of which must be determined experimentally.

The pressure-viscosity coefficient,  $\alpha$ , is a function of both pressure and temperature and is given by the following relation:

$$\alpha(p, T) = \frac{\ln \mu - \ln \mu_0}{p - p_a} = \frac{1}{a_1 + a_2 T + (b_1 + b_2 T) p} \quad (8)$$

The constants  $a_1, a_2, b_1$  and  $b_2$  characterize the behavior of the hydraulic fluid [11].

The values of the constants in Eq. (8) were determined based on experimental data for mineral hydraulic oil with a paraffinic base structure and are given in Tab. 2. [4]

**Table 2. The values of the constants for pressure-viscosity coefficient,  $\alpha$ , for mineral hydraulic oil of paraffinic base structure**

$a_1$ [bar]	$a_2$ [bar/°C]	$b_1$ [–]	$b_2$ [°C <sup>–1</sup> ]
334	3.2557	0.026266	0.000315

As for pressures less than 500 bar,  $a_1 + a_2 T \gg (b_1 + b_2 T) p$ , Eq. (7) can be simplified as Eq. (9):

$$\mu(p, T) = a e^{\left[ \frac{b}{(T+273.15)-c} \right]} e^{\left[ \frac{p}{a_1 + a_2 T} \right]} \quad (9)$$

Fig. 2 shows experimental data for the dynamic viscosity of mineral hydraulic oil HM 46 as a function of temperature and pressure.

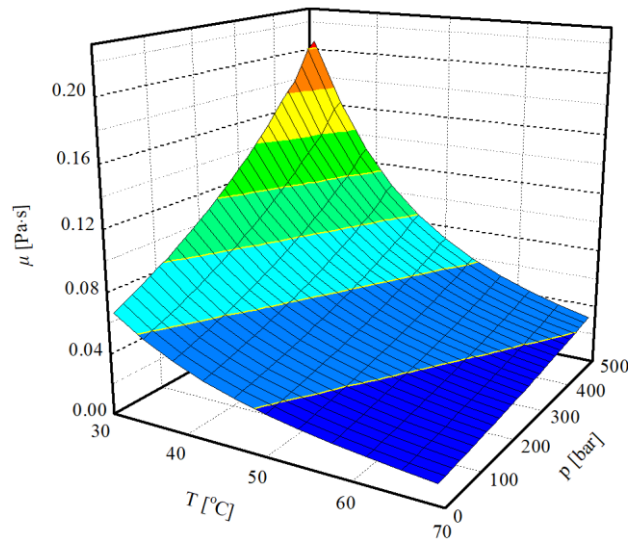


**Figure 2. Variation of dynamic viscosity of mineral hydraulic oil HM 46 on dependance of thermodynamics state**

### 3. Theoretical Determination of the Radial Clearance Flow

Radial clearances can be divided into short ones, where the thermodynamic change in the state of the hydraulic fluid is approximately adiabatic, and long ones, where the thermodynamic change in the state of the hydraulic fluid is approximately isothermal.

Radial clearances can be considered long when the length of boundary layer development within the clearance is much less than the length of overlap, which is the most common case in fluid flow within hydraulic components [12].

Grinding is commonly applied to finish spool surfaces in manufacturing hydraulic components, whereas component body (barrel) surfaces are honed, with a surface quality in accordance with ISO standards, at least N4 (arithmetic mean roughness 0.2  $\mu\text{m}$ ). The test models used for this study's experimental investigations were produced similarly. Since the oil flow through the radial clearances is laminar, the surface roughness of the piston and body (cylinder) does not significantly influence the results.

In this work, experimental measurements were made for long radial clearances (Fig. 3).

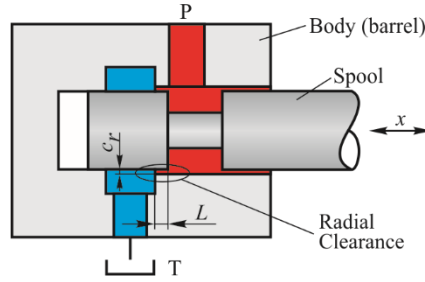


**Figure 3. Long radial clearance**

Considering that the thermodynamic change of the state of the used test fluids is isothermal, the coefficient of dynamic viscosity changes only with changes in pressure. By solving the Navier-Stokes equation, the expression for the flow  $Q$  [m<sup>3</sup>/s] is obtained by Eq (10) [12]:

$$Q = \frac{1 - e^{-\alpha p_0}}{\alpha} \cdot \frac{d_s \pi c_r^3}{12 \mu_0 L} \quad (10)$$

where:

- $p_0$  – pressure at the entrance of the clearance (P) [Pa];
- $d_s$  – diameter of a spool [m];
- $c_r$  – size of radial clearance [m];
- $L$  – length of overlap [m].

#### 4. Experimental Testing Concept

To enable the experimental determination of small flow rates, a test model was developed to evaluate flow through radial clearances - one of the most common types of small openings in hydraulic components. The model consists of two test model bodies (barrels), each equipped with four spools, allowing for the creation of different radial clearance sizes in the range of 5-20  $\mu\text{m}$ .

The experiments were conducted using mineral hydraulic oils of various viscosity grades (ISO VG 22 to ISO VG 68), all belonging to the HM quality class. Due to its low dynamic viscosity coefficient, water was also included in the testing.

Fig. 4 presents the structure of the experimental setup for small flow rate measurements.

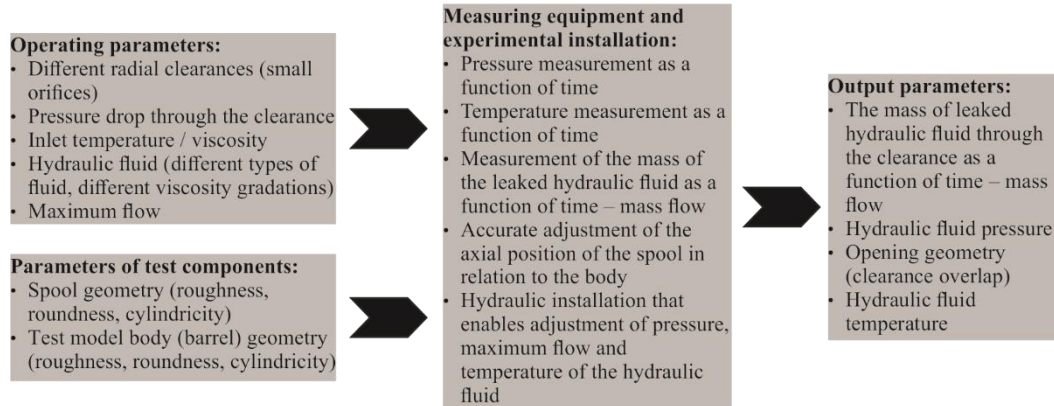


**Figure 4. The structure of the experimental setup for small flow rate measurements**



## 5. Hydraulic System Setup for Experimental Testing

The test installation used for the experimental evaluation is schematically presented in Fig. 5. It comprises several interconnected components that together enable the generation, control, and monitoring of flow through a defined clearance geometry under various operating conditions. It consists of a driving system, a fluid supply unit, a test model, measuring equipment, and a data acquisition system.

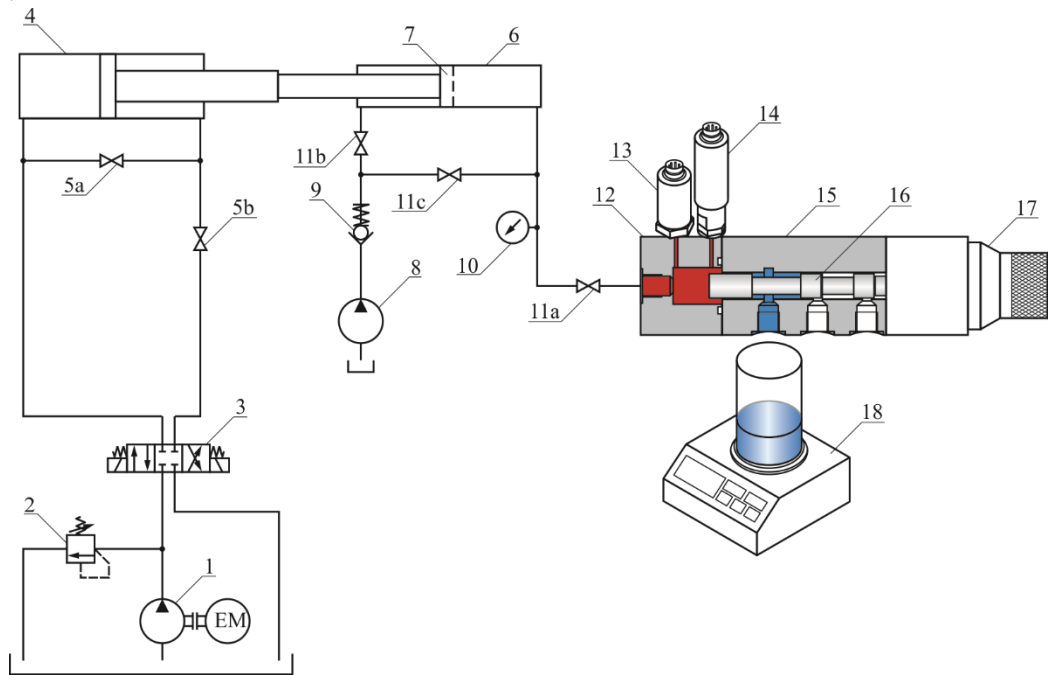


**Figure 5. Measurement installation**

(1-electric motor, 2-pressure relief valve, 3-directional control valve, 4, 6-hydraulic cylinders, 5, 11-manual valves, 7-piston, 8-manual filling unit, 9-non-return valve, 10-pressure gauge, 12-front cover, 13-pressure sensor, 14-temperature sensor, 15-Test model body, 16-spool, 17-rear cover with an indexing mechanism, 18-weighing scale)

The driving system serves to actuate the working hydraulic cylinder. It includes a pump driven by an electric motor (1), a pressure relief valve for regulating the working pressure (2), and a directional control valve (3) used to operate the hydraulic cylinder (4). Two manual valves (5a and 5b) are incorporated to enable the creation of a semi-closed hydraulic circuit, allowing for precise adjustment of the piston speed.

The fluid supply unit, physically separated from the driving system to ensure independent control of input parameters, is composed of a supply cylinder (6) actuated by the hydraulic cylinder (4). Two distinct operating modes are employed: in the first, the piston (7) is removed, allowing only the piston rod to displace the test fluid; in the second, the piston is installed, enabling different flow regimes through the radial clearance and allowing for the determination of the flow coefficient. The supply unit also features a manual filling unit (8) with a non-return valve (9) for introducing test fluid, a pressure gauge (10) for visual monitoring of the inlet pressure, and several manual valves (11a, 11b and 11c) to initiate and control the flow through the clearance.

The picture of the real test model is presented in Fig. 6. The test model comprises:



- a front cover (12) with ports for connecting pressure (13) and temperature (14) sensors and for introducing the test fluid into the radial clearance;
- a test model body (barrel) (15);
- a spool (16) inserted into the test model body to form the radial clearance and
- a rear cover that supports an indexing mechanism (17).

This mechanism enables precise axial positioning and locking of the spool. It allows control over the overlap length of the clearance and ensures stability during measurement.



**Figure 6. Test model assembly with attached sensors**

The measuring equipment includes a pressure sensor (13), a temperature sensor (14), and a high-precision weighing scale (18), which together enable accurate monitoring of the fluid's thermodynamic and flow parameters.

All measuring instruments are connected to a data acquisition system, which consists of a computer used to collect, store, and process the measured data in real time.

## 6. Results of Experimental Tests

Due to the extensive amount of data obtained from the experimental tests, it was not feasible to present all results in this paper. Therefore, a selection of representative examples has been included to illustrate the key findings. The representative examples are presented in Fig 7, Fig. 8, and Fig. 9. The left side of the figures shows the results of mass measurements as a function of time, while the right side presents the measured mass flow rate.

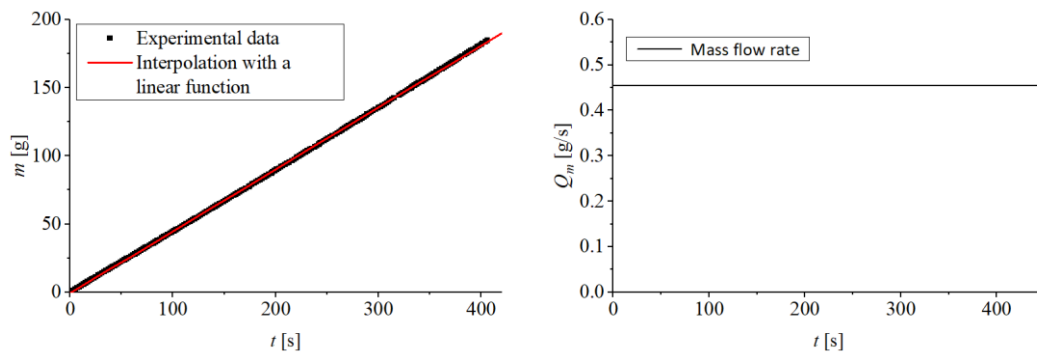


**Figure 7. Piston 10 mm, radial clearance 17  $\mu\text{m}$ , overlap 6 mm, pressure 350 bar, temperature 23  $^{\circ}\text{C}$ , oil HM 46**

Fig. 7 shows the mass flow rate through a radial clearance of  $17\ \mu\text{m}$  at an operating pressure of 350 bar and a lower oil temperature of  $23\ ^\circ\text{C}$ . The figure shows that the flow through the clearance remains constant over the extended measurement period. The measured mass flow rate is  $0.453\ \text{g/s}$  (corresponding to a volumetric flow rate of  $0.031\ \text{L/min}$ ), while the value obtained using Eq. (10) is  $0.028\ \text{L/min}$  (corresponding to a mass flow rate of  $0.413\ \text{g/s}$ ).

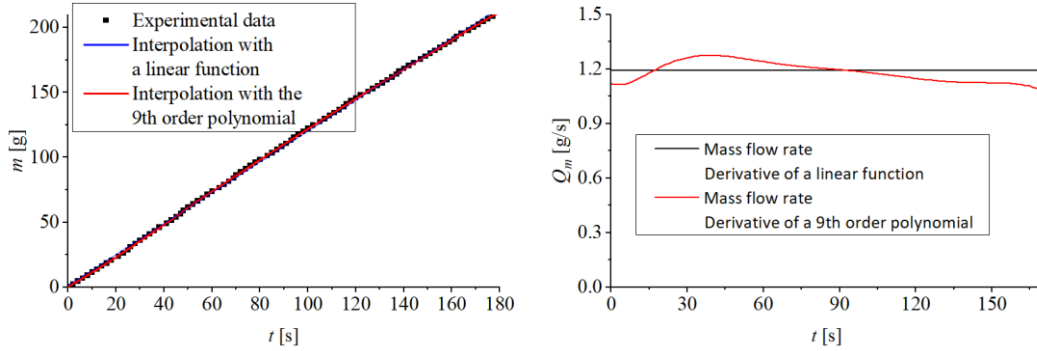


**Figure 8. Piston 10 mm, radial clearance  $17\ \mu\text{m}$ , overlap 10 mm, pressure 350 bar, temperature  $51\ ^\circ\text{C}$ , oil HM 46**

Fig. 8 presents the mass flow measurement through the same clearance size, measured at a pressure of 350 bar and an elevated oil temperature of  $51\ ^\circ\text{C}$ . In this case, the flow through the clearance exhibits minor variations over time and remains approximately constant. The measured mass flow rate is  $1.1\ \text{g/s}$  (corresponding to a volumetric flow rate of  $0.0767\ \text{L/min}$ ), while the value obtained using Eq. (10) is  $0.075\ \text{g/s}$  (corresponding to a volumetric flow rate of  $1.08\ \text{L/min}$ ).

In all cases where clearances can be classified as long, good agreement was achieved between the measured flow rates and the values calculated using Eq. (10).

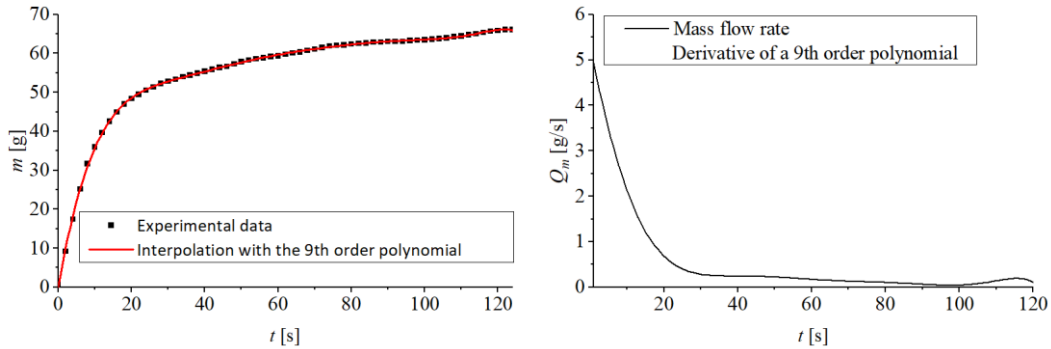


**Figure 9. Piston 10 mm, radial clearance  $7.5\ \mu\text{m}$ , overlap 0.2 mm, pressure 120 bar, temperature  $57\ ^\circ\text{C}$ , oil HM 46**

In Fig. 9, the mass flow measurement through a smaller radial clearance of  $7.5\ \mu\text{m}$  is shown at an operating pressure of 120 bar and a higher oil temperature of  $57\ ^\circ\text{C}$ . The figure shows that the flow through the clearance rapidly decreases over time, eventually stopping altogether. The decrease in mass flow results from the phenomenon of clearance obliteration.

In this case, the application of Eq. (10) does not provide accurate results because it was derived for the flow of hydraulic fluid through long radial clearances, where the change in the fluid state can be

considered isothermal. Here, however, the flow occurs through so-called short radial clearances, where the change in the fluid state is approximately adiabatic.

The available literature has not thoroughly investigated the phenomenon of clearance obliteration (clearance-closing effect), and few studies address this issue. Experimental investigations conducted by the authors of this study indicate that the clearance-closing effect becomes significant for radial clearances smaller than 10  $\mu\text{m}$  and that its intensity increases with higher working fluid temperatures. The significance of these experimental results lies in that existing mathematical models do not account for this phenomenon, as it is nearly impossible to predict without experimental evidence.

Clearance obliteration occurs when the boundary layer within a narrow clearance occupies a substantial portion of the nominal flow cross-section, thereby reducing or even completely blocking fluid passage. Factors such as fluid pressure, temperature, and contaminants influence the intensity of this process. For clearances greater than 20  $\mu\text{m}$ , the effect of gap obliteration becomes negligible and is typically omitted in flow rate calculations [1].

## 7. Conclusions

Based on the conducted experimental investigations and analysis, the following key conclusions can be drawn:

1. Measuring very small flow rates, such as internal leakage, is one of the most challenging tasks in testing hydraulic components.
2. The permissible leakage through small orifices and internal clearances is typically minimal compared to the nominal flow through the main flow paths of hydraulic components.
3. In specific test scenarios, it may be physically impossible to isolate the leakage path, particularly when multiple internal clearances allow fluid to flow from high to low-pressure zones within the component.
4. Experimental results confirm that the accurate determination of small flow rates (leakage) requires detailed knowledge of how the fluid's physical properties – especially viscosity and density – change with temperature and pressure. Inadequate understanding or neglect of these dependencies can lead to significant errors in interpreting test results.
5. The equations used to calculate the flow rate through the radial clearances depend on the length of the overlap between the piston and the body of the component. In this work, the formula for the flow rate is given, and measurements were made for the so-called long radial clearances. The paper presents only typical examples from a large number of measurements for various operating parameters.
6. Experiments have shown that the value of the flow rate calculated using Eq. (10) coincides with the measured value of the flow rate at the beginning of the measurement in all cases. For radial clearances of less than 10  $\mu\text{m}$ , there is a gradual decrease in flow rate, i.e., a phenomenon that can be called “clearance-closing effect” (which can be seen in the example in Fig. 9). In comparison, for radial gaps greater than 20  $\mu\text{m}$ , this effect does not occur. This conclusion is particularly significant because it impacts the design of control valves in hydraulics, necessitating an increase in the required control force to move the valve spool.

7. A similar measuring installation can be used to measure small flows for other geometric shapes, including small orifices and various types of test fluids.

## References

- [1] Dziubak, T., Szczepaniak P., Modelling Internal Leakage in the Automatic Transmission Electro-Hydraulic Controller, Taking into Account Operating Conditions, *Energies (Basel)*, 16 (2023), no. 22, 7667, doi: 10.3390/en16227667
- [2] Ma, W., *et al.*, Modeling and Analysis of Internal Leakage Characteristics of the Internal Curve Motor by a CFD-Based Method, *Processes*, 12 (2024), no. 12, doi: 10.3390/pr12122835
- [3] Ma, W., *et al.*, Study on the leakage mechanism of the valve plate pair of internal curve hydraulic motor, *Advances in Mechanical Engineering*, 17 (2025), no. 6, doi: 10.1177/16878132251346850
- [4] He, D., *et al.*, Effect of vane tip clearance on cavitation and gas–liquid two-phase flow characteristics of high-speed rotary vane pump, *International Journal of Fluid Engineering*, 2 (2025), no. 2, doi: 10.1063/5.0254835
- [5] Peng, Z., *et al.*, Flow Field Modeling and Simulation of High-Speed Gear Pump Considering Optimal Radial and End Clearance, *IEEE Access*, 11 (2023), pp. 64725–64737, doi: 10.1109/ACCESS.2023.3290079
- [6] Szwemin, P., Fiebig, W., The influence of radial and axial gaps on volumetric efficiency of external gear pumps, *Energies (Basel)*, 14 (2021), no. 15, doi: 10.3390/en14154468
- [7] Li, L., Bin Wu, J., Deformation and leakage mechanisms at hydraulic clearance fit in deep-sea extreme environment, *Physics of Fluids*, 32 (2020), no. 6, doi: 10.1063/5.0009913
- [8] Knežević, D., *et al.*, The Influence of Thermodynamic State of Mineral Hydraulic Oil on Flow Rate Through Radial Clearance at Zero Overlap Inside the Hydraulic Components, *Thermal Science*, 20 (2016), Suppl. 5, pp. S1461-S1471, doi: 10.2298/tsci16s5461k
- [9] Stachowiak, G. W., Batchelor, A. W., *Engineering Tribology*, University of Western Australia, Perth, Australia, 2001
- [10] Keith, P., Hodges, B., *Hydraulic Fluids*, Arnold, London, Great Britain, 1996
- [11] Knežević, D., Savić, V., Mathematical Modeling of Changing of Dynamic Viscosity, as a Function of Temperature and Pressure, of Mineral Oils For Hydraulic Systems, *Facta Universitatis*, 4 (2006), pp. 27-34, UDC 532.1:665.6
- [12] Knežević, D., *et al.*, Determination of the Flow Rate Through Long Radial Clearances Inside Hydraulic Components, *Engineering & Automation Problems*, 2 (2012), pp. 23-31, UDC 5.32

Paper submitted: July 7, 2025

Paper revised: July 28, 2025

Paper accepted: August 6, 2025